Characterization of Microstructure with a Scanning Electron Microscope and Energy Dispersive X-ray Spectroscopy

Eman Mousa Alhajji
North Carolina State University
Department of Materials Science and Engineering

MSE 255 Lab Report
203
A
Danial Rasic
3/2/2016

Abstract

JEOL JSM-6010LA Scanning electron microscopy and energy dispersive x-ray spectroscopy were used to examine the microstructure of the alloy and to determine the elemental compositions of the phases present in two mounted Pb-Sn samples and one steel sample. The area ratio of steel pearlite was determined to be 1/9 cementite to ferrite, corresponding to 0.11 wt% C. The large dark areas in steel microstructure were found to be proeutectoid ferrite. The quantitative analysis of lead-tin alloy sample 1 showed that it was 54.7% tin and 45.3% lead for sample 1 and was 89.8% tin and 10.2% lead for sample 2. Sample 1 was found to represent a nearly eutectic (hypoeutectic) structure consisting of tin and lead layers and primary lead–rich phase. In contrary, sample 2 is clearly hypereutectic since the amount of tin exceeded the eutectic point.

Introduction

One of the fundamental goals in using a scanning electron microscope (SEM) for structural analysis is the visualization of microstructures in 3D. In term of examining the microstructures, SEM is very similar to optical microscopy but it is used on a smaller length scale. [1] The SEM provides two outstanding improvements over the optical microscope. First, it extends the resolution limits so that the micrograph magnifications can be increased from 1,000 to >100,000. Second, it improves the depth-of-field resolution by a factor of approximately 300. A primary use of the scanning electron microscope is to produce high resolution and/or high depth-of-field images of sample surfaces. A second use, perhaps equally important, is to provide elemental determination of very small volumes of material. Another advantage of the SEM is the ability for direct observation of the external form of real, complex surfaces, such as fracture surfaces and microelectromechanical (MEMS) devices. Figure 1 shows the basic components of the scanning electron microscope. They can be categorized as: (1) the electron column (the electron gun or source, electron lenses, apertures, scanning coils, and stigmator coils), (2) the specimen chamber, (3) the vacuum pumping system, (4) signal detectors, and (5) electronics and instrument controls including the graphical user interface.

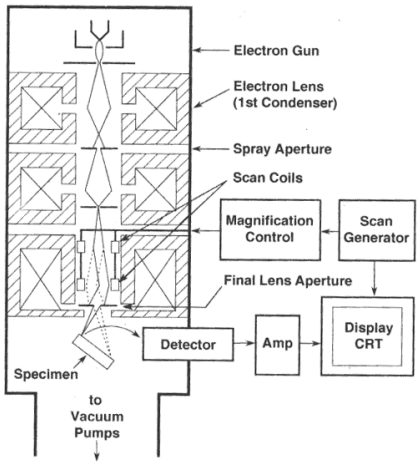

Figure 1. Schematic of the basic components of a scanning electron microscope. [1]

Whereas optical microscopes use optical lenses, electron microscopes typically employ electromagnetic lenses that are comparable to simple solenoid coils. A coil of copper wire in an iron housing produces a magnetic field to produce the lensing action. As an electron moves through the magnetic field, it experiences a radial force inward, which is proportional to the Lorentz force,

$$\vec{\mathbf{F}} = -e(\vec{\mathbf{v}} \times \vec{\mathbf{B}}) \ , \tag{1}$$

where **v** is electron velocity and **B** is magnetic flux density.

In order to make high resolution images, the initial spot from the electron gun has to be demagnified. The smaller the spot size on the sample surface, the higher the potential resolution. Images are formed by scanning the beam over the sample surface using scan coils, which are typically located just above the objective lens. The beam is typically scanned in a raster pattern. The ratio of the scanned area to the displayed area determines the magnification, i.e., the smaller the scanned the higher the magnification. Essentially, the beam is placed at a point on the sample, and then signal is collected with an appropriate detector and assigned to the corresponding point on the imaging screen (computer monitor).[2] This process is repeated for all of the points in the raster. Modern digital SEMs can have variable raster sizes where the user will choose the number of pixels desired. Some systems allow the user to specify how many points they wish in both X and Y.[1]

When an electron beam strikes a solid, a variety of signals can be produced that include electrons that both exit the surface and are absorbed by the sample, x-rays, and photons. There are two general types of electron scattering in a solid: elastic and inelastic. Elastic scattering results in a direction change for the primary electron with no loss in energy such as Backscattered electrons (BSE) . Inelastic scattering events result in a transfer of energy from the primary electron to the solid with no change in direction such as Secondary electrons (SE). Backscattered electrons

have an energy that is close to the incident beam energy. Since the probability of backscattering is a function of material density and nuclear size, BSE images will show compositional contrast. Materials with higher average atomic numbers will appear brighter (more BSEs emitted) and lower average atomic number materials will appear dark. Topographic contrast is minimized with a BSE detector. Secondary electrons and X-rays are the result of inelastic scattering events. The pulse processor sorts the X-rays by energy. The SE detector will produce images that consist of mostly topographic contrast with some compositional contrast produced by line of sight BSEs. X-ray spectra are typically displayed as a graph of X-ray energy vs. number of counts. The bremsstrahlung will form a background upon which characteristic X-ray peaks will appear. EDS can allow for both qualitative determination of the elements in the sample and quantitative determination of amount of an element present. [2]

In this lab, JEOL JSM-6010LA scanning electron microscope was used to examine pearlite in order to determine area ratio of ferrite to cementite and to understand contrast differences between phases and grain size in Pb/Sn alloy via backscattering electron and secondary electron modes. It was also used to evaluate the chemical composition of the phases in the specimens using Energy Dispersive X-ray Spectroscopy (EDXS).

Experimental procedure

Using JEOL JSM-6010LA scanning electron microscope, the microstructures of three specimens were examined: Pearlite and two Pb/Sn alloy samples. The software used to generate the data was in touch scope. SE, BSE and EDXS were performed. In BSE, Solid state detectors are a Si diode that creates electron-hole pairs when struck by an electron with sufficient energy, which is usually >3keV. The electron-hole pairs are swept apart by an applied bias. In both SE and EDXS, when the X-ray strikes the detector, electron-hole pairs are produced that are swept

apart by a bias applied to the contacts. The number of electron-hole pairs produced is proportional to the energy of incident X-ray. [1]

First, the samples were placed in the chamber of the JEOL JSM-6010LA scanning electron microscope. The samples were handled with gloves, but they were exposed to air and had experienced surface attire and tear from use. The experiment was operated at room temperature. The accelerating voltage was 20.0kV, and the pressure was 3.7×10-7 Torr. Second, the stage position was adjusted using the XY knobs and note the specimen position and height. 9. For the sample holders, the top of the holder was in the same plane as the working distance of 10 mm when the Z axis was set to 10 mm. The initial focusing was completed by regulating the working distance, which is the distance between the lens and the samples. The image resolution was further advanced by stigmation correction. Using wobble, this correction was used to eliminate electrons far from the main axis of the electron beam by passing it through an asymmetric electric field to force it to be round. Then the spots were demagnified in order to increase the resolution. The magnification at which the images were taken was 2000 times. Brightness and contrasts were adjusted as appropriate to each sample. For the EDS imaging mode, the operating ranges for the death-time of the x-rays were between 20 and 40% in order to maximize the output and prevent high energy exposure. The operating ranges for capturing were 3,000 to 30,000 captures per second. The chamber camera was turned off to prevent the contribution of unwanted signals. The images were formed by scanning sport sizes of 50 for the secondary electron and backscattered images and 60 for the energy dispersive x-ray images. Singles were collected on signal with respect to XY position. The ratio of ferrite to cementite was calculated using an image editor called GIMP.

The following are the abbreviations used in the micrographs and what they stand for: SEI-Secondary electron image, BEC – Backscattered Electrons, kV – Energy of incident beam, WD – working distance and SS – Spot Size.

Results

SEM images were taken for steel and two samples of tin-lead alloys. The resolution of the images were fairly high. Figure 2 shows the microstructure of plain carbon steel in both SE and BSE images. The dark areas correspond to ferrite phase and the light areas correspond to cementite phase. The black spots are due to vacancies. The area ratio was determined to be 1/9 cementite to ferrite, corresponding to 0.11 wt% C. Using the phase diagram of steel, the large dark areas were found to be proeutectoid ferrite.[3] Regions having the alternating light and dark lamellar structure were determined to be pearlite. The results agree with the literature; the microstructures of alloys having carbon content less than the eutectoid (hypoeutectoid) are comprised of proeutectoid ferrite phase in addition to pearlite.[3] The SE image, as shown in Figure 2, is more effective in determining the area ratio and analyzing the surfaces of steel because SE single contains mostly topographical information about the sample.[1]

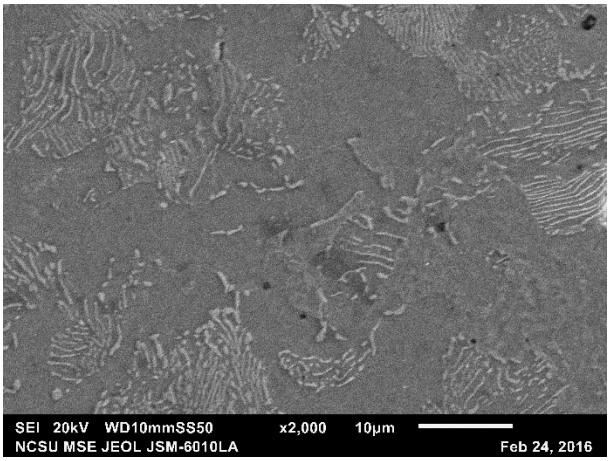

(a)

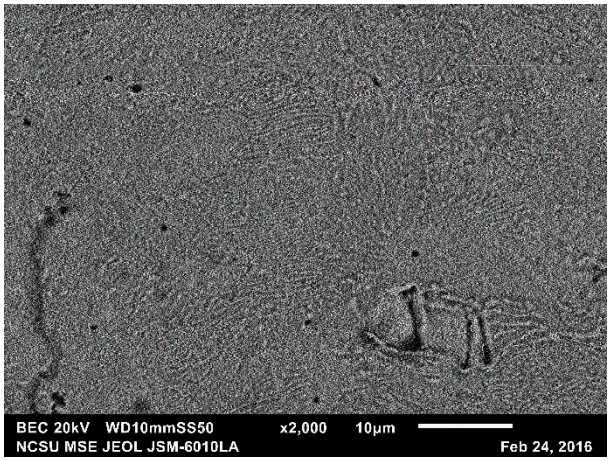

(b)

Figure 2. Microstructure of Steel generated by a Scanning Electron Microscope (a) Secondary Electrons image and (b) Backscattered Electrons image.

Figure 3 shows the microstructure of Lead-Tin Alloy Sample 1 where (a) represents an image using SE signal and (b) represents an image using BSE signal. This microstructure was found to be composed roughly equally of lead and tin. The dark spots correspond to tin-rich phase and the light spots to lead-rich phase.

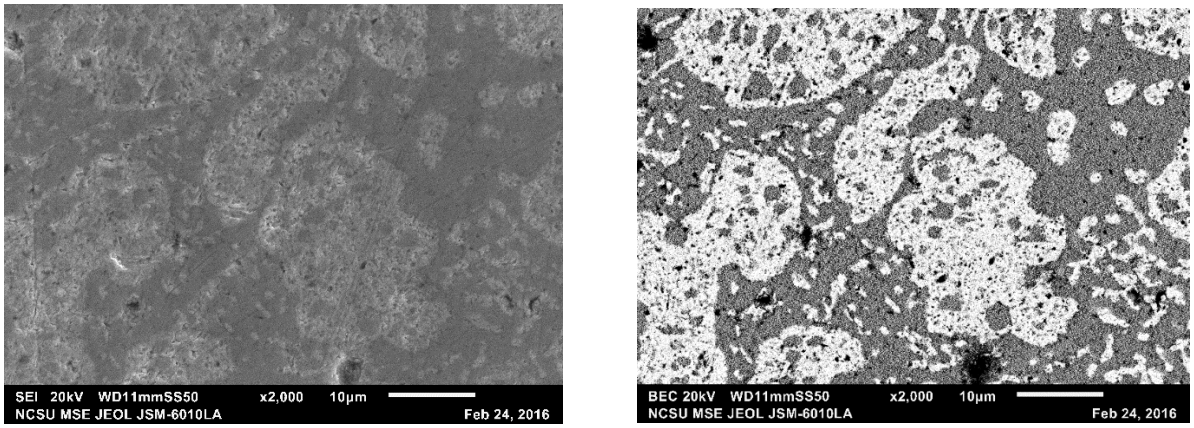

(a) (b)

Figure 3. Microstructure of Lead-Tin Alloy Sample 1 generated by a Scanning Electron Microscope (a) Secondary Electrons and (b) Backscattered Electrons.

Figure 4 shows the EDXS of Lead-Tin sample 1 where (a) represents the Number of X-rays Emitted and Energy, and (b) represent the area composed of Lead in red and Tin in green. The quantitative analysis of this sample showed that it was 54.7% tin and 45.3% lead.

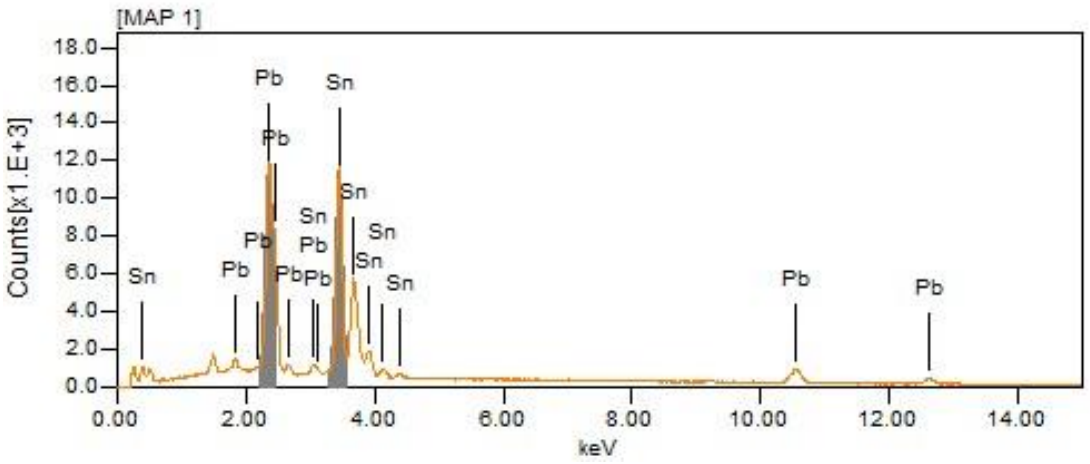

(a)

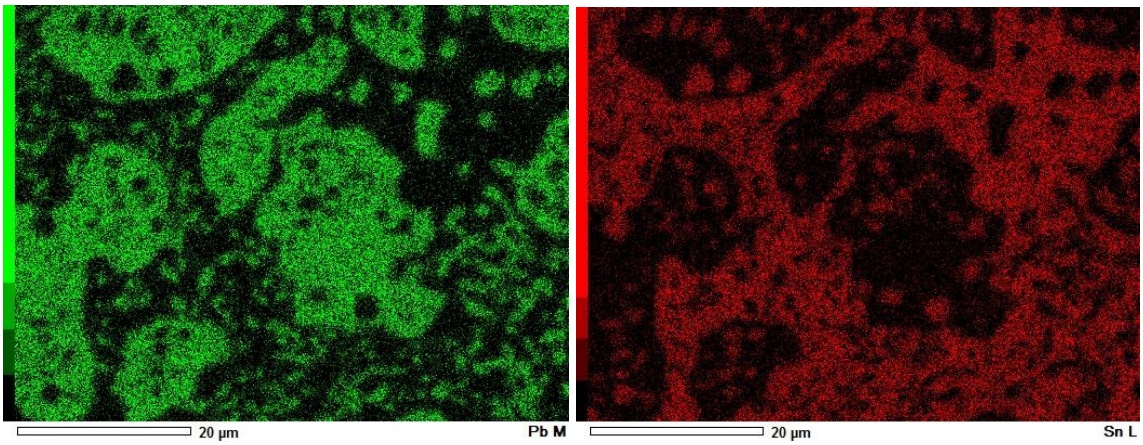

(b)

Figure 4: Energy Dispersive X-ray Spectroscopy of Lead-Tin Sample 1. (a) Number of X-rays Emitted and Energy, and (b) area composed of Lead (Green) and Tin (Red).

The second lead-tin alloy sample was found to have a different composition and plot of the x-ray count and energy. The microstructure of the second sample of lead-tin alloy was observed to be composed mostly of tin as shown in Figure 5. The dark spots correspond to tin-rich phase and the light spots to lead-rich phase. The number of X-rays emitted and energy in distinctive of tin was found to be the majority compare to the one for lead, as shown in Figure 6.

The quantitative analysis of this sample generated by EDS showed that it was 89.8% tin and 10.2% lead.

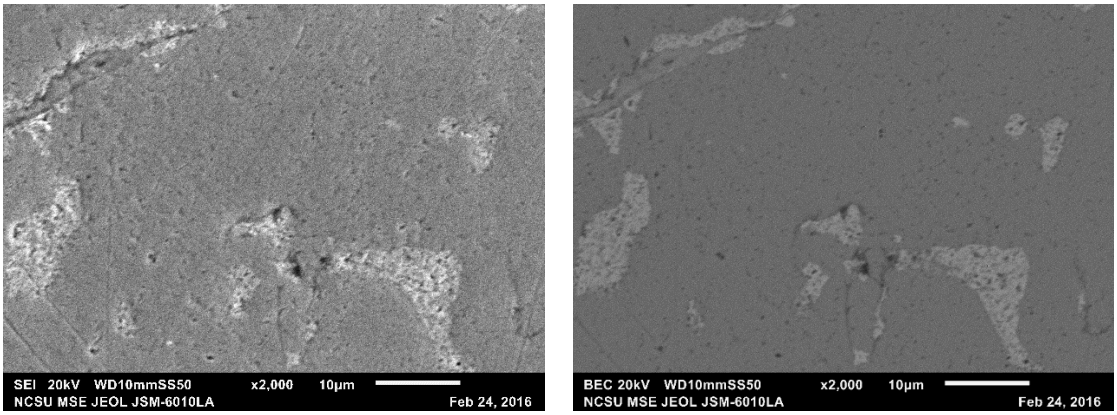

(a) (b)

Figure 5. SEM images of Microstructure of Lead-Tin Alloy Sample 2 generated (a) Secondary Electrons and (b) Backscattered Electrons.

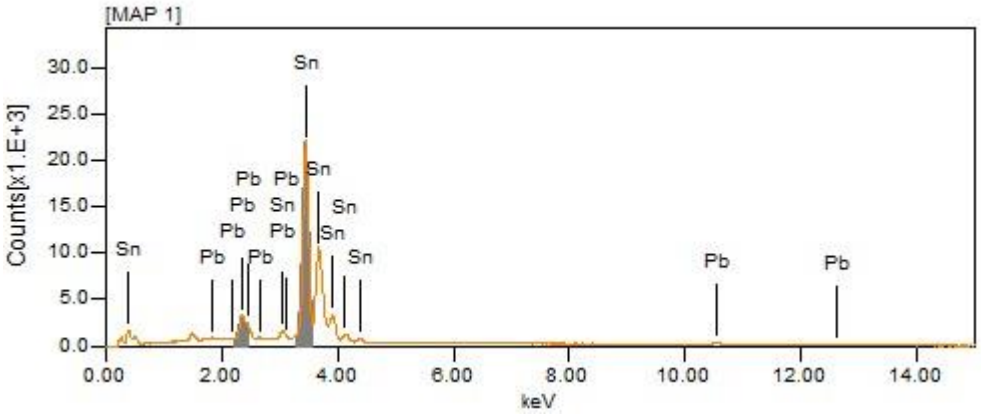

(a)

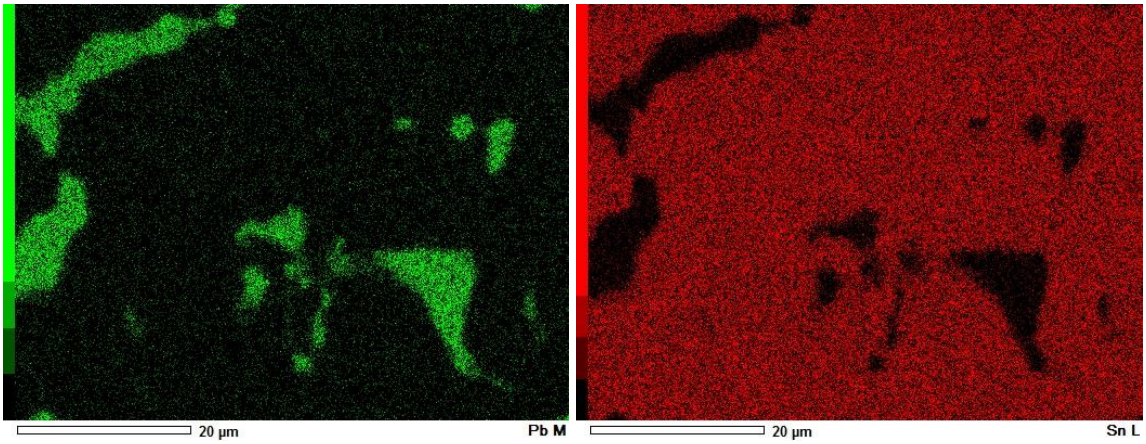

(b)

Figure 6: Energy Dispersive X-ray Spectroscopy of Lead-Tin Sample 1. (a) Number of X-rays Emitted and Energy, and (b) area composed of Lead (Green) and Tin (Red).

The microstructures of lead-tin alloy samples were compared with the phase diagram of lead-tin alloy and then the relative amounts of lead-tin were estimated.[3] Sample 1 was found to represent a nearly eutectic (hypoeutectic) structure consisting of tin and lead layers and primary lead–rich phase. In contrary, sample 2 is clearly hypereutectic since the amount of tin exceeded the eutectic point. The structure of sample 2 composed of primary tin-rich phase within some lamellar eutectic structure. The data and the analysis agrees with the phase diagram of lead-tin alloy, where the eutectic point occurs at 61.9 wt% Sn.[3] Furthermore, the implications drawn from the BSE micrographs of lead-tin samples agree with the data analysis obtained by XEDS. The BSE images, as shown in Figure 3 and Figure 5, are more effective than SE in determining the compositions of each substance since BSE signals depends on the size of the atom and the volume. [1,3]

Conclusions

In this lab, JEOL JSM-6010LA scanning electron microscope was used to examine pearlite in order to determine area ratio of ferrite to cementite and to understand contrast differences between phases and grain size in Pb/Sn alloy via backscattering electron and secondary electron modes. It was also used to evaluate the chemical composition of the phases in the specimens using Energy Dispersive X-ray Spectroscopy (EDXS).

The secondary electron mode was the most effective mode in determining the topographical information in steel sample. In contrast, the backscattered electron was the most effective in determining the composition of lead-tin alloy samples. Elements with more atomic mass emit more electrons; therefore they are appear brighter. The EDXS was very useful in obtaining numerical analysis of each composition.

The experiment succeed in identifying the microstructure and the composition of each sample using the appropriate mode. For the steel sample, the area ratio of pearlite was determined to be 1/9 cementite to ferrite, corresponding to 0.11 wt% C. The large dark areas in steel microstructure were found to be proeutectoid ferrite. The quantitative analysis of lead-tin alloy sample 1 showed that it was 54.7% tin and 45.3% lead for sample 1 and was 89.8% tin and 10.2% lead for sample 2. Sample 1 was found to represent a nearly eutectic (hypoeutectic) structure consisting of tin and lead layers and primary lead–rich phase. In contrary, sample 2 is clearly hypereutectic since the amount of tin exceeded the eutectic point.

References

[1]. C. Mooney, Scanning Electron Microscopy: A Practical Introduction, MSE 255 Course Locker.

[2]L. Reynolds, Cold roll and anneal of Cu, MSE 255 experiment description, 2016.

[3] W.D. Callister Jr., Materials Science and Engineering: An Introduction, Seventh Edition (Wiley, New York, 2007).